

Electronic Supplementary Information

Asymmetric Binuclear Ni(II) And Cu(II) Schiff Base Metallopolymers

Sara Realista,^a Ana S. Viana,^a Bernardo de P. Cardoso,^a Ana M. Botelho do Rego,^b Pedro D. Vaz,^{a,c} Ana I. Melato^{*a}, Paulo N. Martinho^{*a} and Maria José Calhorda^{*a}

^a Centro de Química e Bioquímica, DQB, Faculdade de Ciências, Universidade de Lisboa, 1749-016 Lisboa, Portugal

^b Centro de Química-Física Molecular (CQFM) and Institute of Nanoscience and Nanotechnology (IN), Instituto Superior Técnico, Universidade de Lisboa, Av. Rovisco Pais, 1049-001 Lisboa, Portugal

^c ISIS Neutron & Muon Source, Rutherford Appleton Laboratory Chilton, Didcot, Oxfordshire OX11 0QX, United Kingdom

*Email: aimelato@ciencias.ulisboa.pt (A.I.M.); pnmartinho@ciencias.ulisboa.pt (P.N.M.); mjcalhorda@ciencias.ulisboa.pt (M.J.C.)

Contents

Synthesis	2
NMR	4
HR-ESI/MS	6
FTIR	8
DFT	9
Cyclic Voltametry	12
AFM	14
XPS	14

Synthesis of A. Salicylaldehyde (0.106 mL, 1 mmol) was added to a solution of potassium bicarbonate (0.200 g, 1 mmol) in ethanol (8 mL). After stirring for 15 min, a solution of nickel(II) acetate tetrahydrate (0.144 g, 0.5 mmol) in ethanol (8 mL) was added dropwise to the mixture and the green solution was stirred for 30 min at rt. 3,3'-diaminobenzidine (0.107 g, 0.5 mmol) was dissolved in hot ethanol (13 mL) and added dropwise to the green solution. The mixture was stirred overnight at reflux and a dark brown solid was filtered and washed with cold ethanol (10 mL) and diethyl ether (10 mL). Yield: 94 %. **IR** (KBr, ν/cm^{-1}): 3378, 3272 ($\nu_{\text{w}}, \nu_{\text{NH}_2}$), 3007, 3070 ($\nu_{\text{w}}, \nu_{\text{C-Harom}}$); 1606 (s, $\nu_{\text{C=N}}$); 1617, 1523 (m, $\nu_{\text{C=Carom}}$); 757 (m, $\delta_{\text{C-Harom}}$). **¹H NMR** (400 MHz, DMSO- d_6 , 298 K) δ/ppm : 9.01 (s, 1H, H-C=N), 8.81 (s, 1H, H-C=N), 8.22 (s, 1H, Ar-H), 8.10 (d, $J = 8.7$ Hz, 1H, Ar-H), 7.67 (d, $J = 7.7$ Hz, 1H, Ar-H), 7.59 (d, $J = 7.9$ Hz, 1H, Ar-H), 7.46 (d, $J = 8.7$ Hz, 1H, Ar-H), 7.32 (t, $J = 7.81$ Hz, 1H, Ar-H), 7.30 (t, $J = 7.91$ Hz, 1H, Ar-H), 6.98 (s, 1H, Ar-H), 6.94 (d, $J = 8.2$ Hz, 1H, Ar-H) 6.90-6.87 (m, 2H, Ar-H), 6.68 (t, $J = 7.81$ Hz, Ar-H), 6.66 (t, $J = 7.91$ Hz, 1H, Ar-H), 6.62 (d, $J = 8.2$ Hz, 1H, Ar-H), 4.75 (s, 2H, NH₂), 4.56 (s, 2H, NH₂). **¹³C NMR** (100 MHz, DMSO- d_6 , 298 K) δ/ppm : 165.2 (Ar-O), 164.9 (Ar-O), 156.5 (C=N), 155.4 (C=N), 142.8 (C), 141.2 (C), 140.2 (C), 135.1, 134.9 (CH), 134.2 (CH), 134.0 (CH), 127.3 (C), 124.8 (CH), 120.4 (C), 120.3 (C), 120.2, 120.1 (CH), 116.5 (CH), 116.0 (CH), 115.2 (CH), 114.4 (CH), 112.7 (CH), 112.2 (CH). **Anal. Found (calcd)** for C₂₆H₂₀N₄NiO₄·0.5C₂H₅OH·1.5H₂O (506.18): C 61.97 (61.69) H 4.18 (4.58) N 11.20 (11.07).

Synthesis of B. According to procedure described for **A**, complex **B** was obtained from salicylaldehyde (0.106 mL, 1 mmol) and potassium bicarbonate (0.200 g, 1 mmol) in ethanol (8 mL), copper(II) acetate monohydrate (0.100 g, 0.5 mmol) in ethanol (8 mL) and 3,3'-diaminobenzidine (0.107 g, 0.5 mmol) in ethanol (13 mL). Yield: 93 %. **IR** (KBr, ν/cm^{-1}): 3345, 3281 (w, ν_{NH_2}), 3051, 3011 (w, $\nu_{\text{C-Harom}}$); 1609 (s, $\nu_{\text{C=N}}$); 1585, 1525 (s, $\nu_{\text{C=Carom}}$); 757 (m, $\delta_{\text{C-Harom}}$). **Anal. Found (calcd)** for C₂₆H₂₀CuN₄O₂·0.7H₂O (496.44): C 62.70 (62.90) H 4.12 (4.34) N 11.10 (11.29).

Synthesis of 1. A solution of nickel(II) acetate tetrahydrate (0.071 g, 0.25 mmol) in ethanol (5 mL) was added dropwise to a ethanolic solution of 3,5-di-*tert*-butylsalicylaldehyde (0.117 g, 0.5 mmol). This mixture was stirred at reflux and after 30 min a hot solution of **A** (0.120 g, 0.25 mmol) in dimethylformamide (10 mL) was added dropwise. A few drops of phosphoric acid were added and the mixture was left for 48 h at 120 °C. The solution was filtered and the precipitate washed with dichloromethane and the desired crude product recovered as filtrate. The filtrate was evaporated in vacuum and the solid washed with *n*-hexane. The solid was redissolved in dichloromethane filtered and evaporated to give a redish brown product. Yield: 58 %. **IR** (KBr, ν/cm^{-1}): 3051 (w, $\nu_{\text{C-Harom}}$); 2950, 2903, 2885 (m, ν_{CH_3} and CH); 1610 (s, $\nu_{\text{C=N}}$); 1584, 1545 (s, $\nu_{\text{C=Carom}}$); 1358 (m, δ_{CH_3}); 753 (w, $\delta_{\text{C-Harom}}$). **¹H NMR** (400 MHz, DMSO- d_6 , 298 K) δ/ppm : 9.09 (s, 1H, H-C=N), 9.00 (s, 1H, H-C=N), 8.93 (s, 1H, H-C=N), 8.85 (s, 1H, H-C=N), 8.54 (s, 1H, Ar-H), 8.50 (s, 1H, Ar-H), 8.27 (d, $J = 9.0$ Hz, 1H, Ar-H), 8.24 (d, $J = 8.6$, 1H, Ar-H), 7.86 (d, $J = 8.6$, 1H, Ar-H), 7.81 (d, $J = 9.0$, 1H, Ar-H), 7.66-7.63 (m, 2H, Ar-H), 7.49 (s, 1H, Ar-H), 7.47 (s, 1H, Ar-H), 7.36 (s, 2H, Ar-H), 7.35-7.31 (m, 2H, Ar-H), 6.93-6.90 (m, 2H, Ar-H), 6.71-6.67 (m, 2H, Ar-H), 1.42 (s, 18H, C(CH₃)₃), 1.30 (s, 18H, C(CH₃)₃). **¹³C RMN** (100 MHz, DMSO- d_6 , 298 K) δ/ppm : 165.3, 165.2 (Ar-O), 163.3, 163.2 (Ar-O), 156.9 (C=N), 156.7 (C=N), 156.4 (C=N), 156.1 (C=N), 142.9 (C-N), 142.7 (C-N), 142.2 (C-N), 141.9 (C-N), 138.1 (C), 137.3 (C), 135.2, 135.1 (CH), 134.2 (CH), 129.7 (CH), 127.6 (CH), 126.3 (CH), 125.7 (CH), 120.3 (CH), 120.3 (C), 119.8, 119.7 (C), 116.2 (CH), 115.9 (CH), 115.3 (CH), 114.0 (CH), 113.8 (CH), 35.4 (C(CH₃)₃), 33.7

(C(CH₃)₃), 31.1 (CH), 29.6 (C(CH₃)₃). **Anal. Found (calcd)** for C₅₆H₅₈N₄Ni₂O₄·0.7H₂O·0.25C₃H₇NO (999,36): C 68.32 (68.20) H 6.33 (6.17) N 5.82 (5.96).

Synthesis of 2. According to procedure described for **1**, complex **2** was obtained from copper(II) acetate monohydrate (0.05 g, 0.25 mmol) in ethanol (5 mL), 3,5-di-*tert*-butylsalicylaldehyde (0.117 g, 0.5 mmol) in ethanol (5 mL) and **B** (0.121 g, 0.25 mmol) in dimethylformamide (10 mL). Yield: 42 %. **IR** (KBr, v/cm⁻¹): 3005 (w, ν_{C-Harom}); 2954, 2904, 2851 (m, ν_{CH₃} and CH); 1612 (s, ν_{C=N}); 1583, 1524 (s, ν_{C=Carom}); 1384 (m, δ_{CH₃}); 756 (m, δ_{C-Harom}). **HR-MS (ESI):** Calcd for C₅₆H₅₉Cu₂N₄O₄ [M+H]⁺ m/z = 977.3123, found m/z = 977.3113. **Anal. Found (calcd)** for C₅₆H₅₉Cu₂N₄O₄·1.1H₂O·0.1C₃H₇NO (1008.13): C 67.31 (67.15) H 6.37 (6.21) N 5.56 (5.72).

Synthesis of 3. A mixture of 3,5-di-*tert*-butylsalicylaldehyde (0.234 g, 1 mmol) and 3,3'-diaminobenzidine (0.021 g, 0.1 mmol) in ethanol (13 mL) was stirred at reflux for 5 h. After 5 h, a solution of nickel(II) acetate tetrahydrate (0.057 g, 0.2 mmol) in ethanol (5 mL) was added dropwise and the mixture was left at reflux for 12 h. The crude product was filtered and washed with *n*-hexane. The solid was dissolved in chloroform, the solution was filtered and evaporated in vacuum to give a red solid as final product. Yield: 90 %. **IR** (KBr, v/cm⁻¹): 3003 (w, ν_{C-Harom}); 2954, 2905, 2868 (s, ν_{CH₃} and CH); 1617 (s, ν_{C=N}); 1581, 1524 (s, ν_{C=Carom}); 1385 (m, δ_{CH₃}); 787 (m, δ_{C-Harom}). **¹H NMR** (400 MHz, acetone-d₆, 298 K) δ/ppm: 8.89, 8.76 (s, 4H, H₁, H₅), 8.51 (s, 2H, H₆), 8.18, 7.76 (d, 4H, H₇, H₈), 7.48-7.40 (m, 8H, H₂, H₃, H₄), 1.50, 1.33 (s, 18H, *tert*-butyl groups). **Anal. Found (calcd)** for C₇₂H₉₀N₄Ni₂O₄·C₂H₆O (1237.58): C 71.41 (71.76) H 7.71 (7.80) N 4.88 (4.53).

Synthesis of 4. According to procedure described for **3**, complex **4** was obtained from 3,5-di-*tert*-butylsalicylaldehyde (0.234 g, 1 mmol) and 3,3'-diaminobenzidine (0.021 g, 0.1 mmol) in ethanol (13 mL) and copper(II) acetate monohydrate (0.040 g, 0.2 mmol) in ethanol (5 mL). Yield: 93 %. **IR** (KBr, v/cm⁻¹): 3039 (w, ν_{C-Harom}); 2997, 2955, 2905 (s, ν_{CH₃} and CH); 1615 (s, ν_{C=N}); 1581, 1522 (s, ν_{C=Carom}); 1357 (m, δ_{CH₃}); 789 (m, δ_{C-Harom}). **HR-MS (ESI):** Calcd for C₇₂H₉₁Cu₂N₄O₄ [M+H]⁺ m/z = 1201.5627, found m/z = 1201.5626. **Anal. Found (calcd)** for C₇₂H₉₁Cu₂N₄O₄ (1202.60): C 71.63 (71.91) H 7.66 (7.54) N 4.60 (4.66).

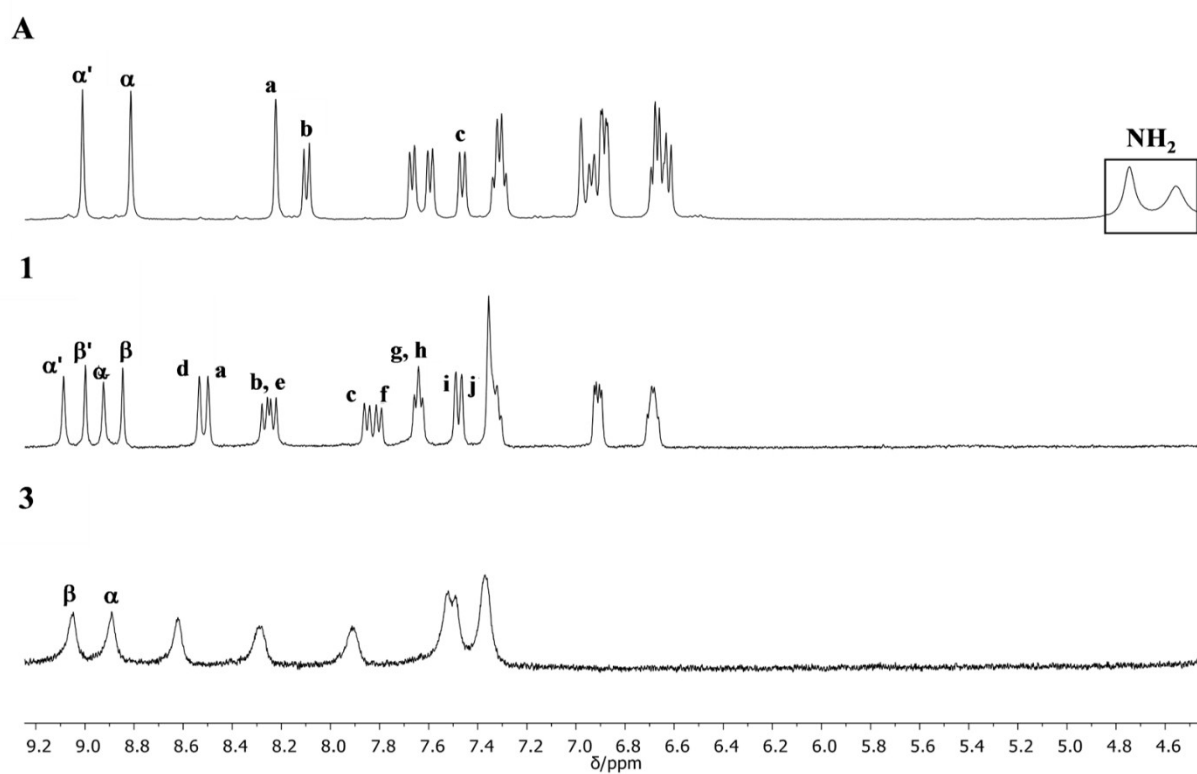


Figure S1. ^1H NMR spectra (DMSO- d_6) of complexes A, 1 and 3.

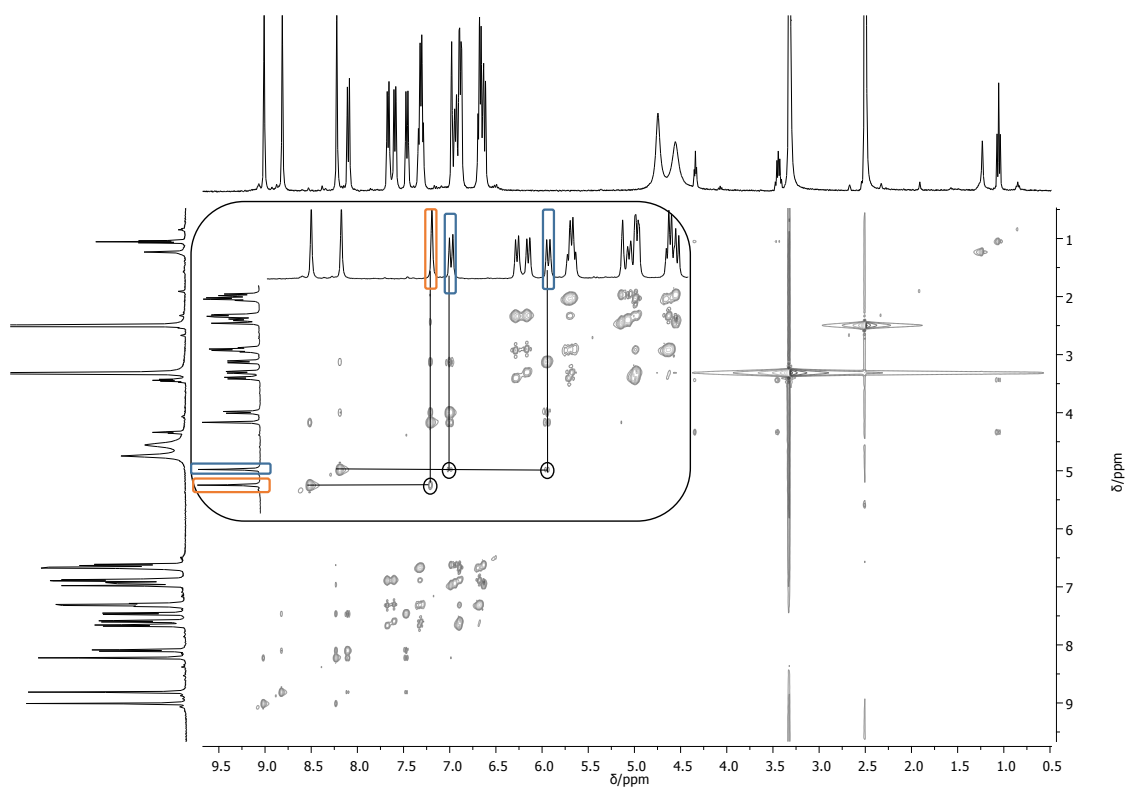


Figure S2. 2D TOCSY (d_6 -DMSO) spectrum of complex A. Inset: Detailed correlation with the imine protons and DAB subunit protons.

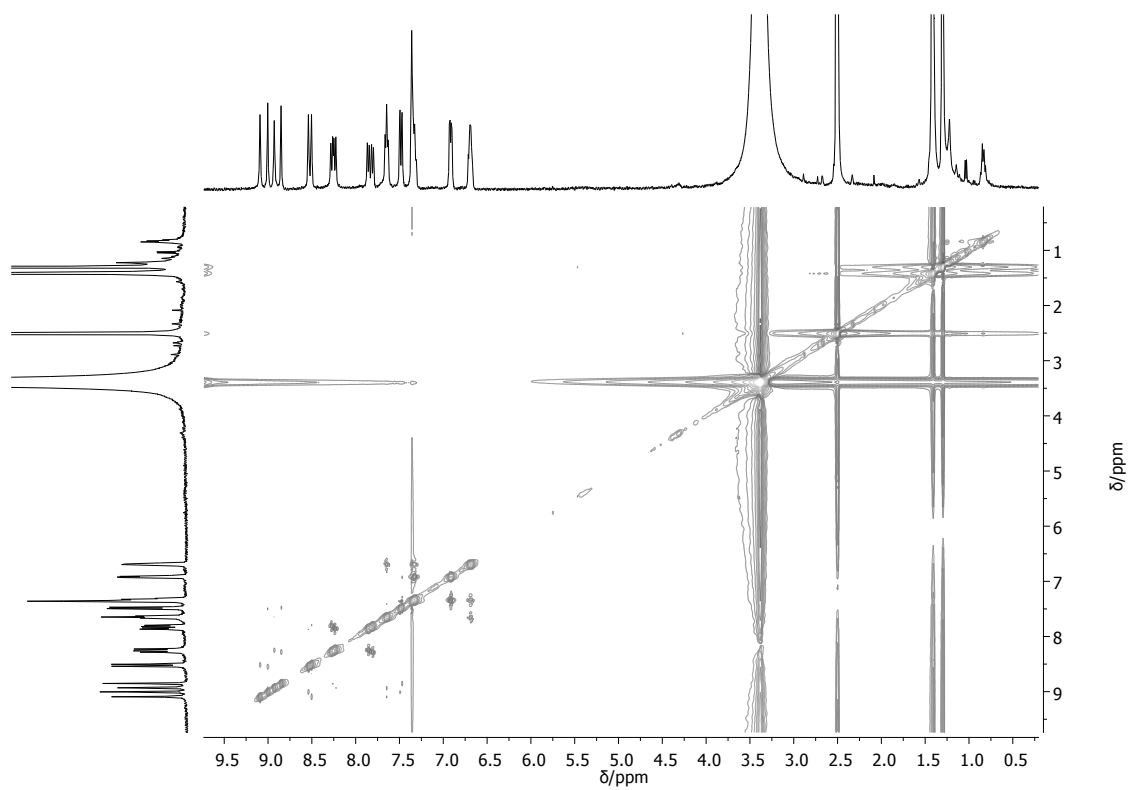


Figure S3. 2D TOCSY d_6 -DMSO spectrum of complex **1**.

Display Report

Analysis Info		Acquisition Date	
Analysis Name	D:\Data\GEMAB 2013-07-30\SQR112b_full_000003.d	7/30/2013 12:30:38 PM	
Method	ESI_Pos_IRMPD_20100616	Operator	
Sample Name	SQR112b	Instrument	apex-Qe
Comment	Full MS		

Acquisition Parameter					
Polarity	Positive	Source	ESI	No. of Laser Shots	1
Averaged Scans	32	No. of Cell Fills	1	Laser Power	0.0 %
Broadband Low Mass	889.5 m/z	End Plate	4000.0 V	MALDI Plate	250.0 V
Broadband High Mass	1200.0 m/z	Capillary Entrance	4500.0 V	Imaging Spot Diameter	2000.0 μ m
Acquisition Mode	Single MS	Skimmer 1	20.0 V		
Pulse Program	basic	Drying Gas Temperature	200.0 $^{\circ}$ C	Calibration Date	Tue Jul 30 11:42:41 2013
Source Accumulation	0.2 sec	Drying Gas Flow Rate	2.0 L/min	Data Acquisition Size	524288
Ion Accumulation Time	2.0 sec	Nebulizer Gas Flow Rate	4.0 L/min	Apodization	Sine-Bell Multiplication
Flight Time to Acq. Cell	0.0 sec				

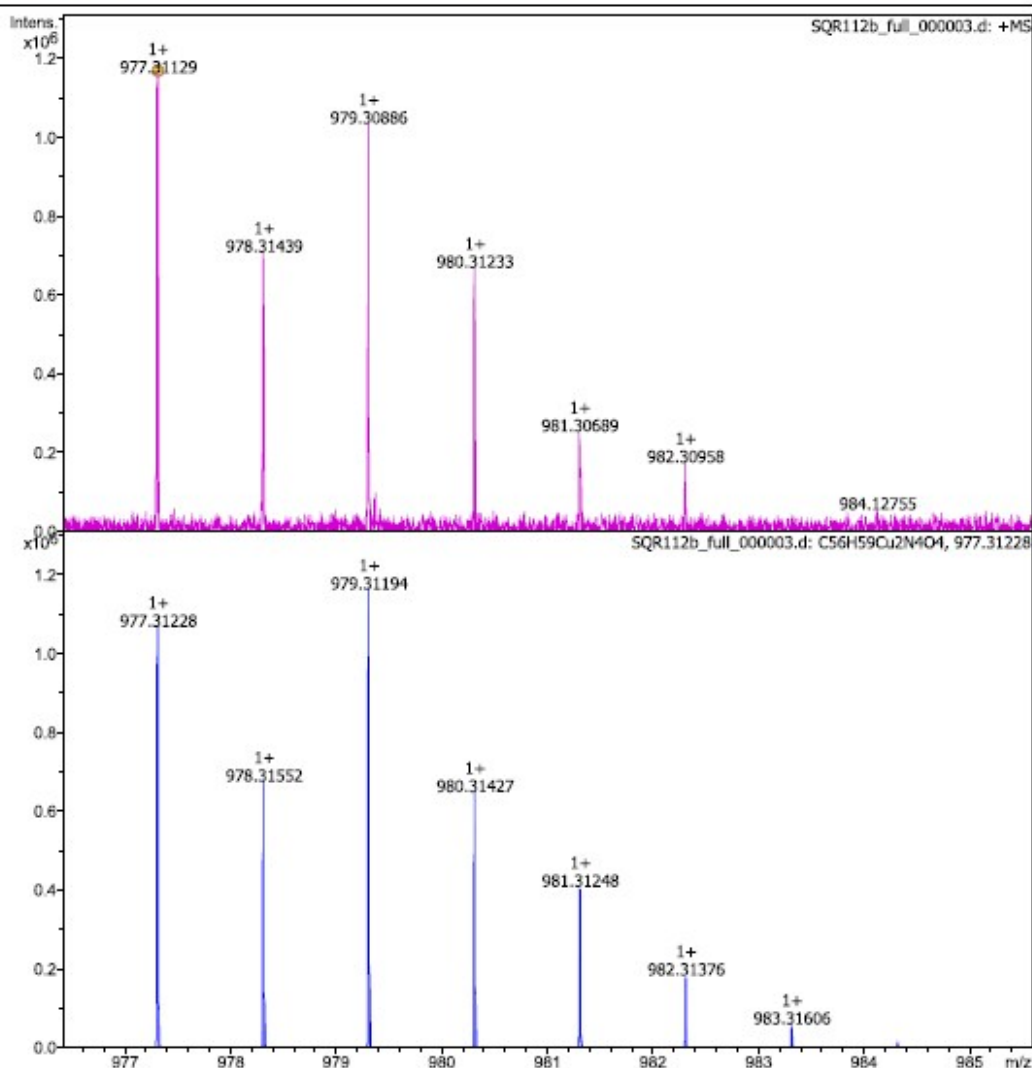


Figure S4. HR-ESI/MS spectrum for complex **2** predicted (bottom) experimental (top).

Display Report

Analysis Info		Acquisition Date	
Analysis Name	C:\Users\pmvaz\Documents\Pedro\GEMAB\Análises MS\GEMAB 2013-07-30\SQR110_full_000001.d	30-07-2013 16:06:11	
Method	ESI_Pos_IRMPD_20100616	Operator	
Sample Name	SQR110	Instrument	apex-Qe
Comment	Full MS		

Acquisition Parameter					
Polarity	Positive	Source	ESI	No. of Laser Shots	1
Averaged Scans	32	No. of Cell Fills	1	Laser Power	0.0 %
Broadband Low Mass	689.5 m/z	End Plate	4000.0 V	MALDI Plate	250.0 V
Broadband High Mass	1400.0 m/z	Capillary Entrance	4500.0 V	Imaging Spot Diameter	2000.0 µm
Acquisition Mode	Single MS	Skimmer 1	20.0 V	Calibration Date	Tue Jul 30 11:42:41 2013
Pulse Program	basic	Drying Gas Temperature	200.0 °C	Data Acquisition Size	524288
Source Accumulation	0.2 sec	Drying Gas Flow Rate	2.0 L/min	Apodization	Sine-Bell Multiplication
Ion Accumulation Time	2.0 sec	Nebulizer Gas Flow Rate	4.0 L/min		
Flight Time to Acq. Cell	0.0 sec				

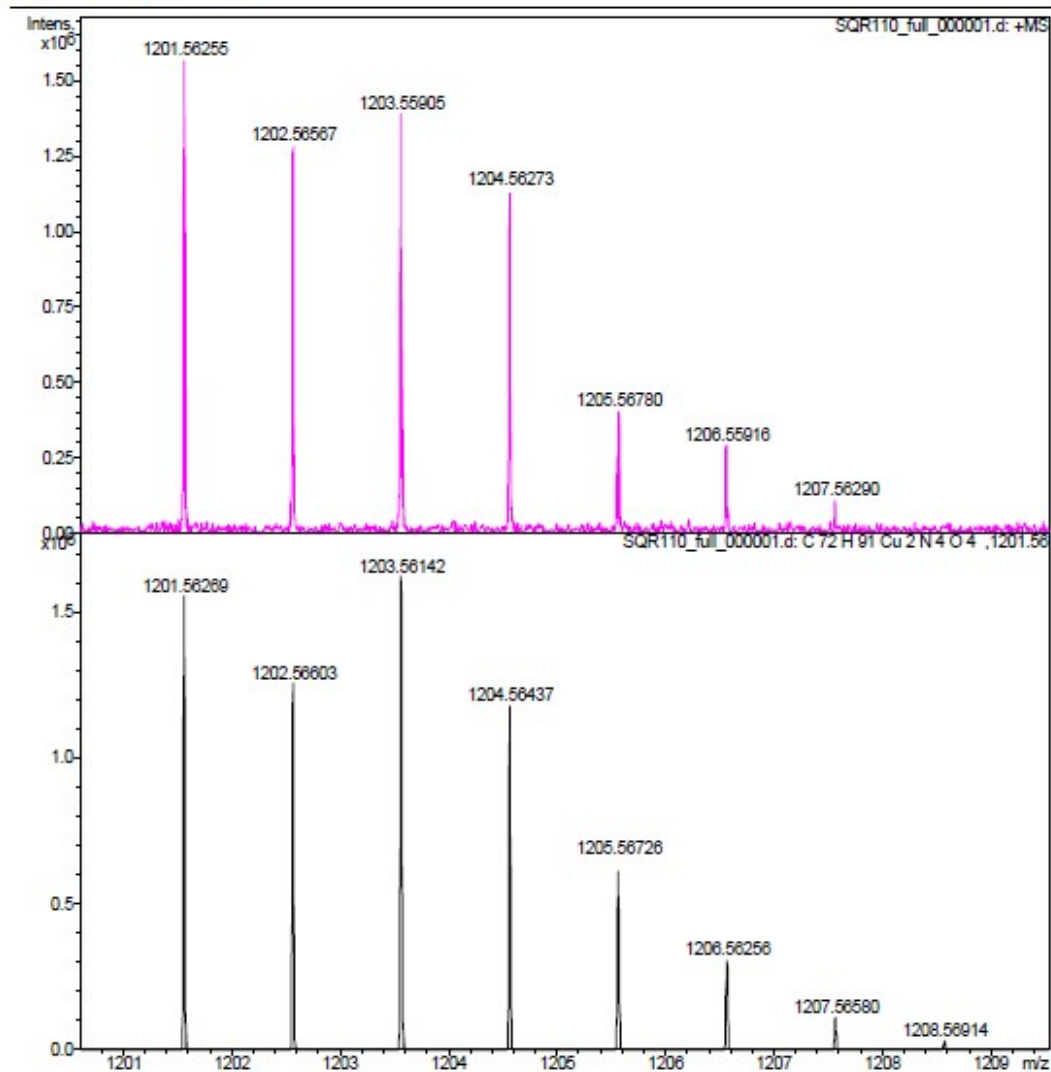


Figure S5. HR-ESI/MS spectrum for complex **4** predicted (bottom) experimental (top).

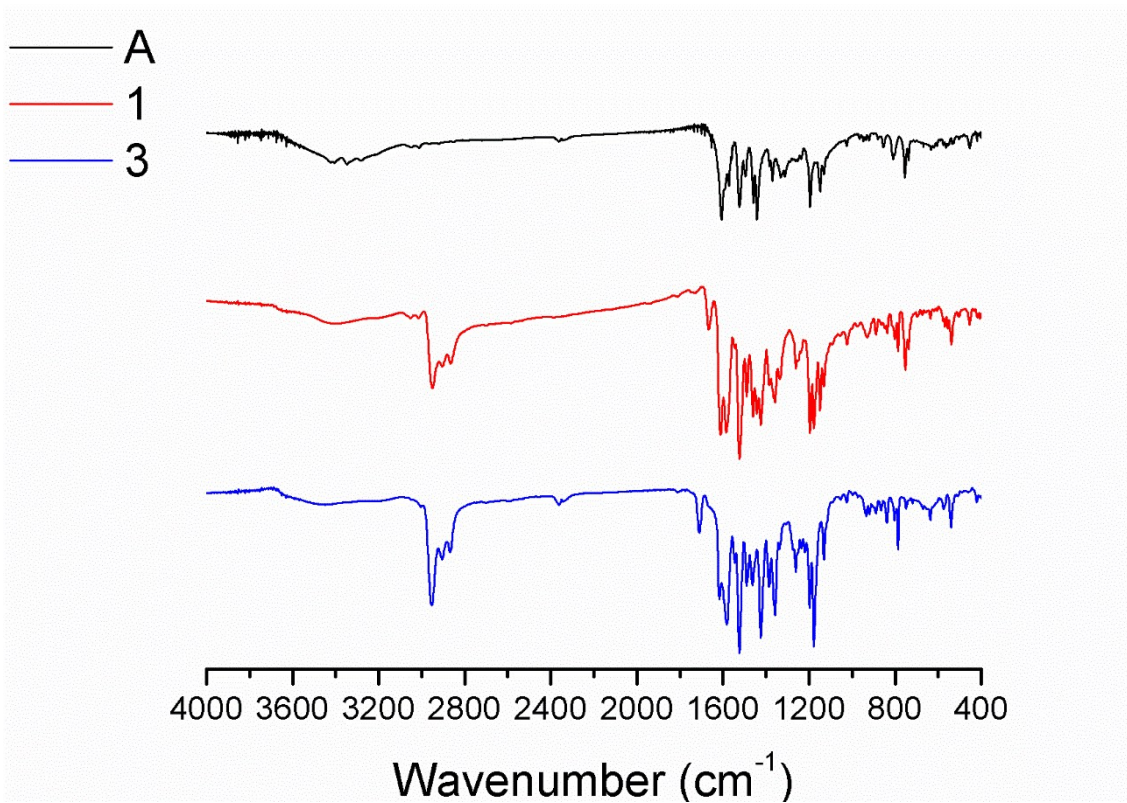


Figure S6. FTIR spectra of Ni(II) complexes.

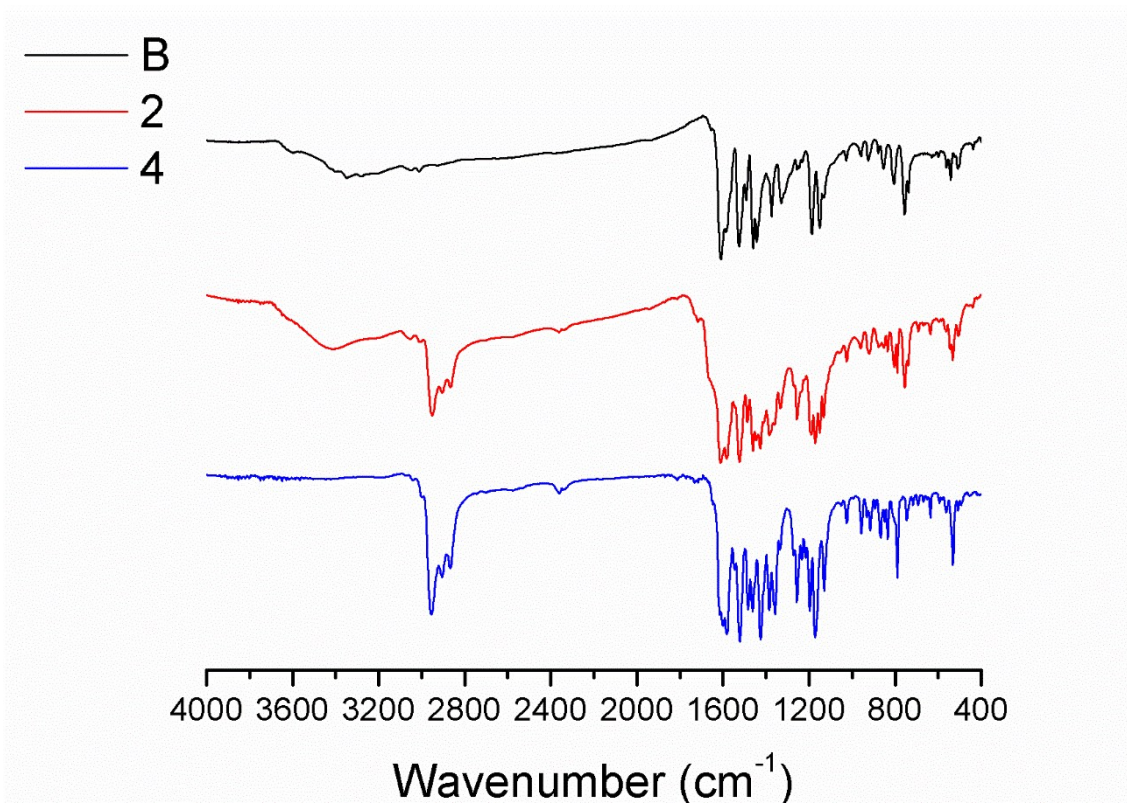


Figure S7. FTIR spectra of Cu(II) complexes.

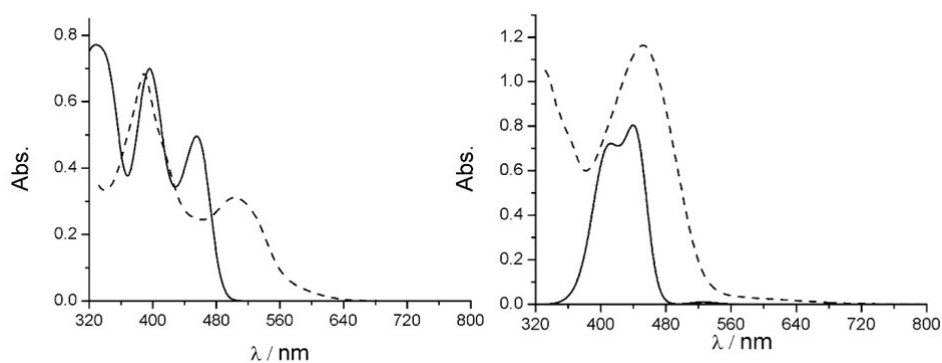


Figure S8. UV-vis spectra of **1** (10^{-5} M, left) and **2** (10^{-6} M, right): in dichloromethane (dashed line), and TD-DFT (solid line, gas-phase).

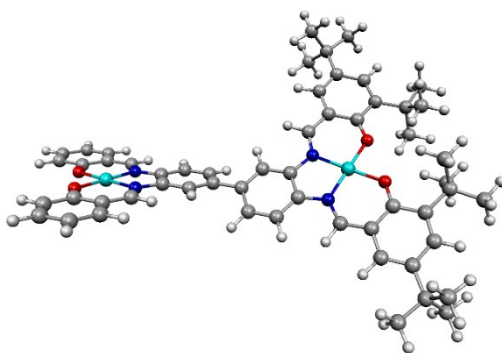


Figure S9. DFT optimised structure of complex **1**.

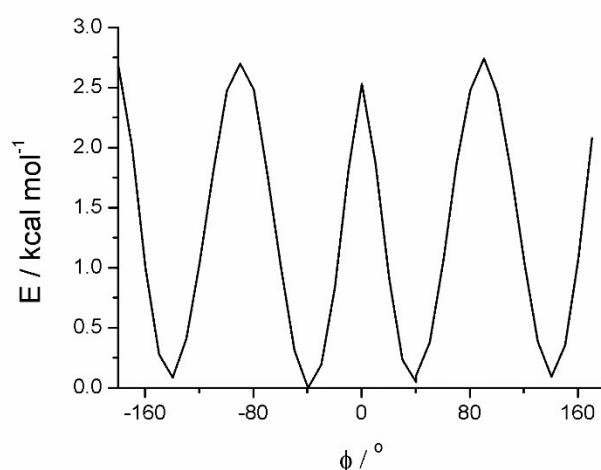


Figure S10. Potential energy scan (kcal mol^{-1}) for varying the dihedral angle, ϕ ($^\circ$), of the biphenyl bridge in the DAB subunit. Energy maxima correspond to orthogonal arrangements of the ligand and minima to $\phi \sim 40^\circ$.

Table S1. Excited states, composition, energy, wavelength and oscillator strength from TD-DFT calculations for complex **1**. Corresponding experimental peak wavelengths presented accordingly.

No.	Composition	Energy (eV)	λ (nm)	λ_{exp} (nm)	Oscillator strength
1	H-7 \rightarrow L+4 (63 %); H-10 \rightarrow L+4 (35 %);	2.04	608	\sim 600	0.0001
2	H-12 \rightarrow L+5 (85 %)	2.08	596		0.0001
3	H \rightarrow L (60 %); H \rightarrow L+1 (25 %)	2.68	462	504	0.3174
4	H-1 \rightarrow L (58 %); H-2 \rightarrow L (21 %)	2.77	444		0.1647
5	H \rightarrow L+2 (19 %); H-1 \rightarrow L+1 (18 %); H \rightarrow L+1 (14 %)	3.08	402	389	0.3456
6	H-3 \rightarrow L (25 %); H-2 \rightarrow L+1 (20 %)	3.20	387		0.2699
7	H-4 \rightarrow L (74 %)	3.57	347	-	0.3543
8	H-5 \rightarrow L+1 (39 %); H-6 \rightarrow L (30 %)	3.94	315		0.2284

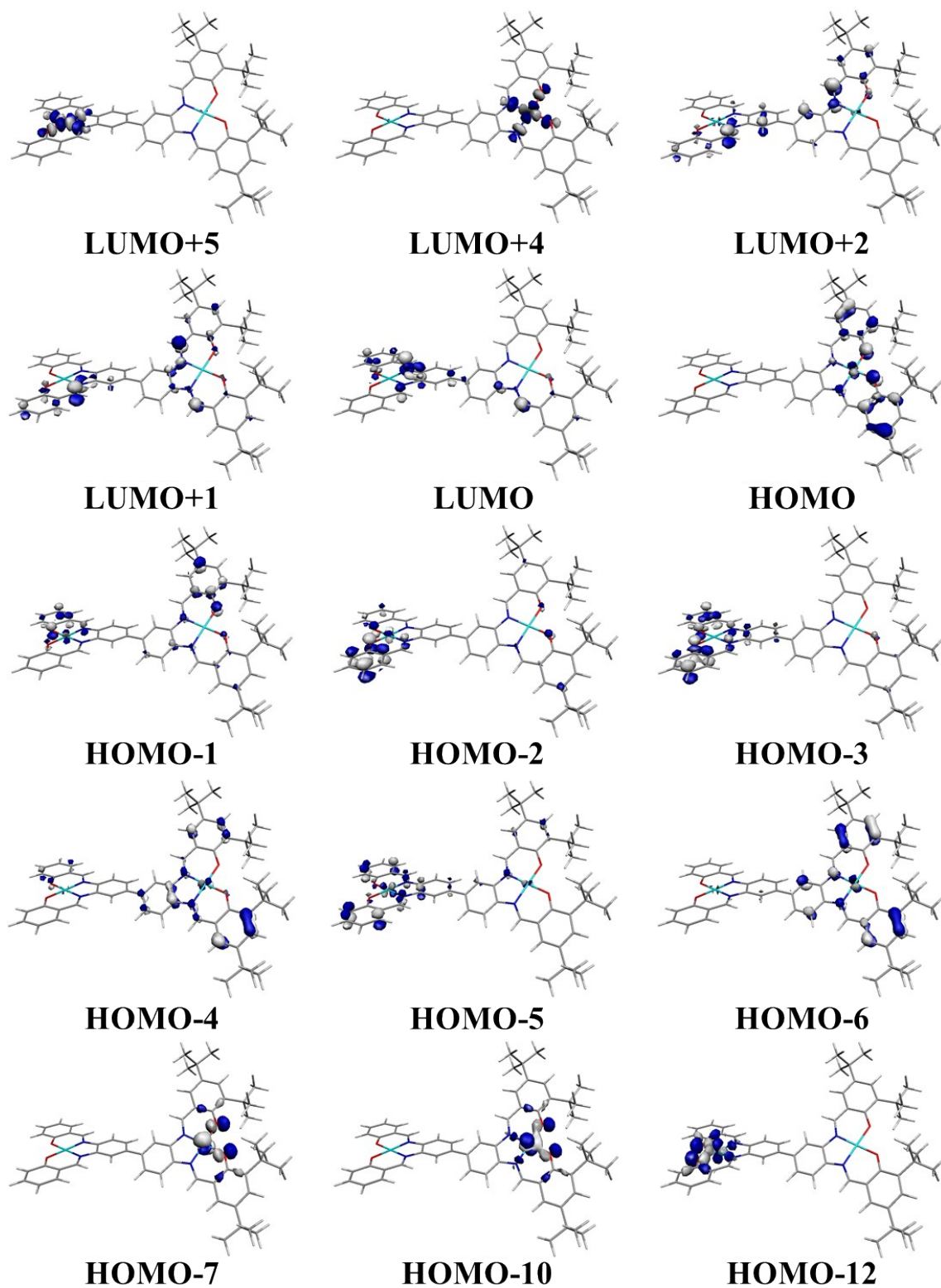


Figure S11. Molecular orbitals of complex 1.

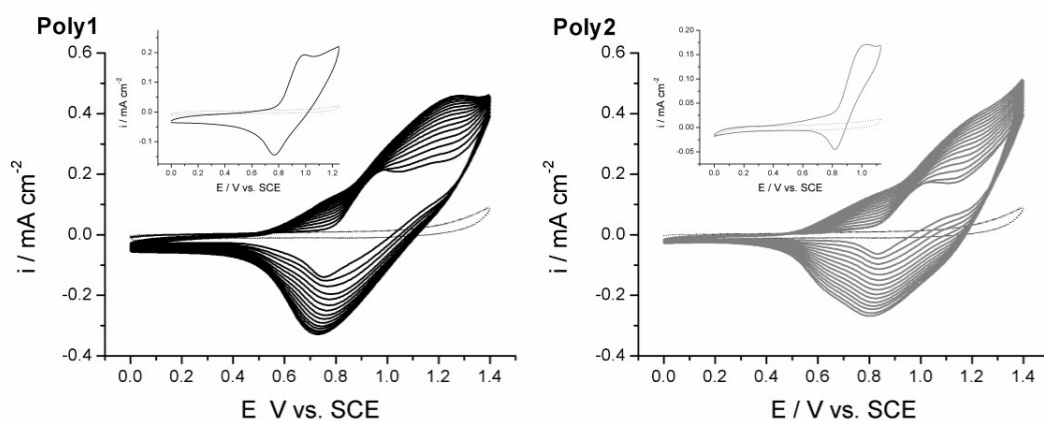


Figure S12. Cyclic voltammograms collected during the potentiodynamic growth of **Poly1** and **Poly2** films on Pt from 1 mM dichloromethane solutions of **1** and **2** using 0.1 M TBAPF₆ as supporting electrolyte (dotted line), $\nu = 50 \text{ mV s}^{-1}$, 15 cycles.

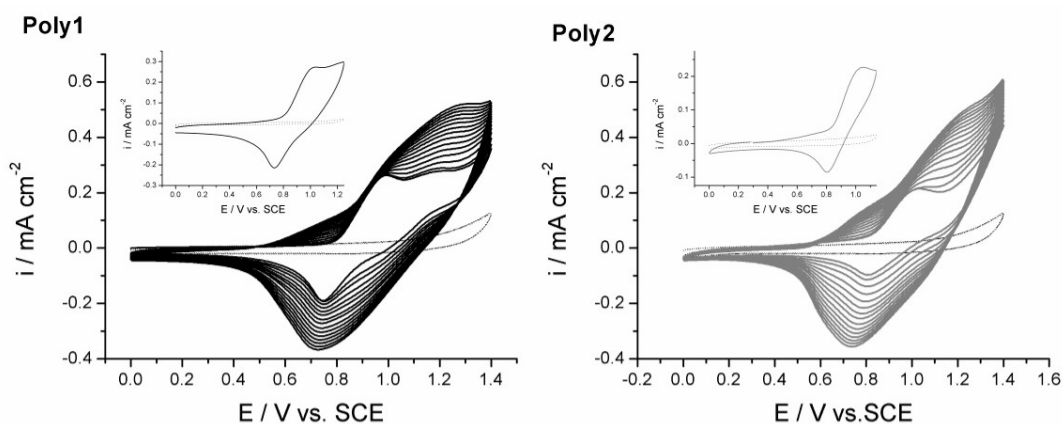
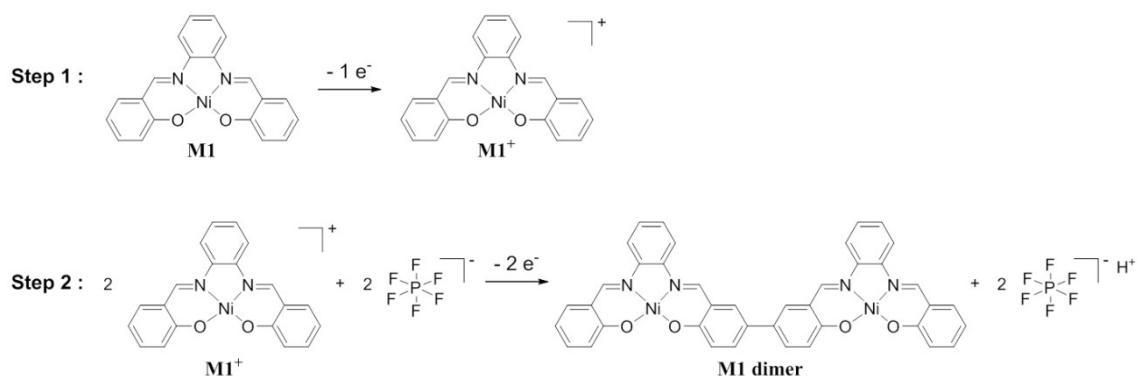


Figure S13. Cyclic voltammograms collected during the potentiodynamic growth of **Poly1** and **Poly2** films on Pt from 1 mM dichloromethane solutions of **1** and **2** using 0.1 M TBAPF₆ as supporting electrolyte (dotted line), $\nu = 100 \text{ mV s}^{-1}$, 15 cycles.



Scheme S1. Two step model dimerization reaction: oxidation of the monomer (Step 1) and formation the new C-C bond with release of protons in the presence of [PF₆]⁻ (Step 2).

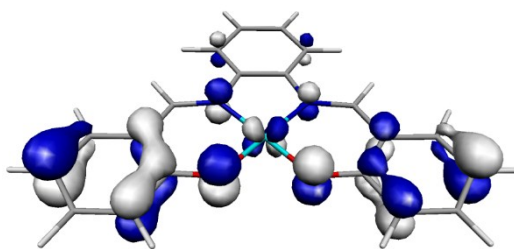


Figure S14. Representation of the SOMO of the $M1^+$ model.

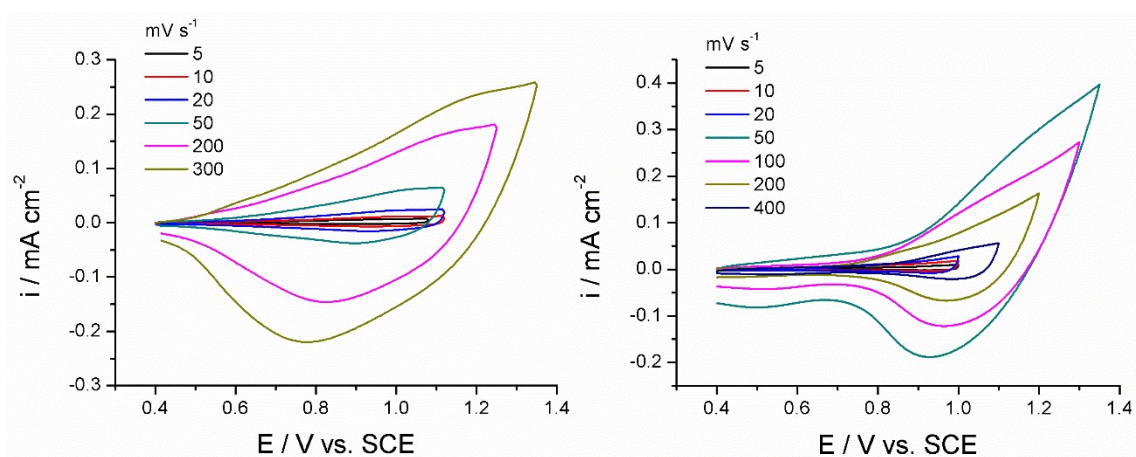


Figure S15. Redox behaviour of **Poly1** (left) and **Poly2** (right) at different scan rates both polymerised at 200 mV s^{-1} .

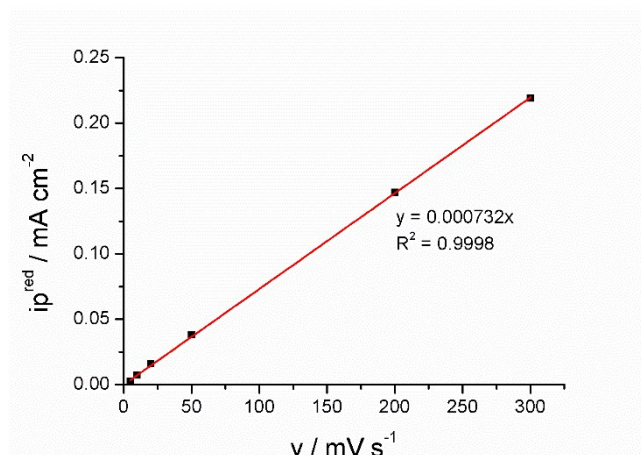


Figure S16. Relationship between reduction peak current and scan rate for **Poly1** grown at 200 mV s^{-1} .

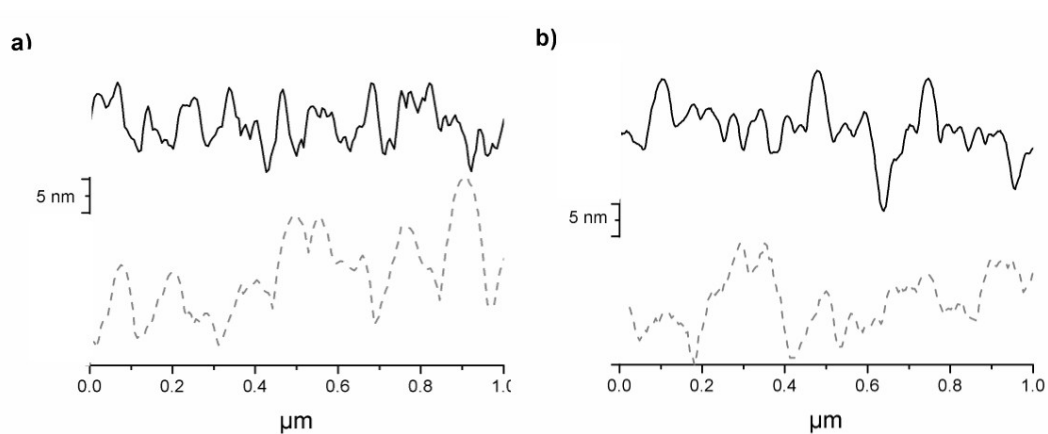


Figure S17. Topographic profiles of **Poly1** (black line) and **Poly2** (dashed line) grown at a) 50 and b) 100 mV s^{-1} .

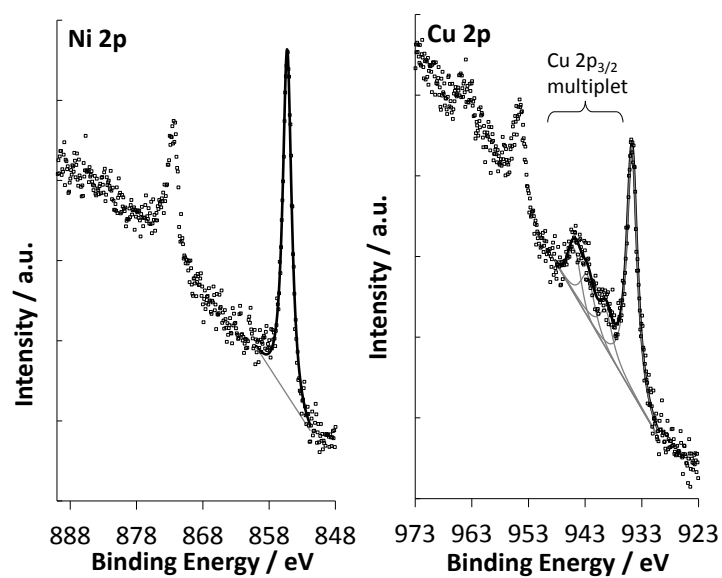


Figure S18. XPS spectra for Ni 2p and Cu 2p in Poly1 (left) and Poly2 (right).